Characterization of zinc-containing catalysts by ^{67}Zn solid-state NMR

Spectroscopic background: ^{67}Zn nuclei have a spin of I = 5/2 and a quadrupole moment of Q = 15.0 x 10^{-30} m^2. Therefore, ^{67}Zn NMR signals of zins atoms in solids are affected by quadrupolar interactions. Additionally, the shape of ^{67}Zn solid-state NMR signals may be slightly affected by anisotropic chemical shielding. The ^{67}Zn isotope has a natural abundance of 4.10 %, a resonance frequency of ν_0 = 31.29 MHz at B_0 = 11.75 T, and a sensitivity of 2.9 x 10^{-3} in comparison with ^{1}H nuclei (1.0). Often, the low resonance frequency of ^{67}Zn nuclei is not in the range of standard solid-state NMR probes. In this case, a specific low-frequency NMR probe is required for ^{67}Zn solid-state NMR investigations. Due to the low sensitivity of ^{67}Zn nuclei, an isotopic enrichment is beneficial for a study of rare zinc species in solids. For basic principles of solid-state NMR, see lectures “Solid-State NMR Spectroscopy” for Bachelor students or PhD seminars, accessible via the link “Lectures for Students”.

ZnO in the pure state and as clusters or guest compounds on support materials and on porous catalysts is one of the zinc compounds, which were early studied by ^{67}Zn solid-state NMR spectroscopy [1, 2].

Fig. 1 shows static ^{67}Zn spin-echo NMR (a) and ^{67}Zn MAS NMR (b) spectra of pure

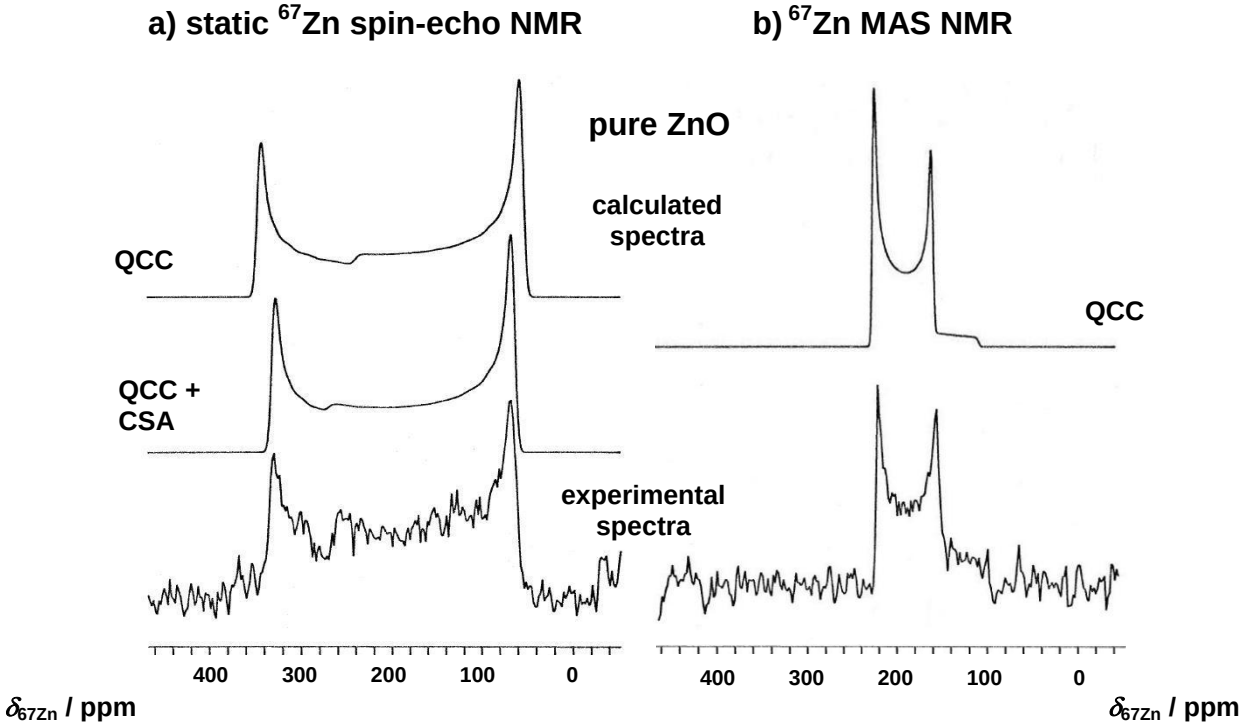

Fig. 1

ZnO powder with natural abundance of ^{67}Zn nuclei and recorded at a magnetic field of B_0 = 9.4 T [2]. These spectra consist of typical powder patterns arising from the central transition of I = 5/2 nuclei in the presence of second-order quadrupole interaction. The wurtzite structure of ZnO crystals is a hexagonal lattice in which the zinc atoms are in tetrahedral coordination with four oxygen atoms (ZnO_4). The best fit of the static ^{67}Zn spin-echo NMR spectrum in **Fig. 1a** was obtained for a quadrupole coupling constant of C_Q = 2.40 MHz and δ_{iso} = 240 ppm (QCC) as well as by including a ^{67}Zn chemical shift tensor (CSA) of δ_{11} = 270 ppm, δ_{22} = δ_{33} = 225 ppm [2]. These results were in excellent agreement with those of the single-crystal ^{67}Zn solid-state NMR study in Ref. [1] and of the more recent studies in Ref. [3].

The effect of doping of ZnO particles with indium, followed by a sintering at T = 1273 to 1373 K, was studied by ^{67}Zn MAS NMR at a magnetic field of B_0 = 18.8 T in Ref. [4]. Similar to the results in Refs. [1] and [2], quadrupole coupling constants of C_Q = 2.40 to 2.47 MHz and δ_{iso} values of 237 to 238 ppm were determined for the pure ZnO material. Upon doping with indium, only a slight increase of the quadrupole coupling constant to C_Q = 2.60 MHz was found, which indicates that the added indium atoms exist as clusters inside the ZnO particles.

In Ref. [5], the transformation of a pressed and sintered (T = 1473 K for 12 h) 3 : 1 mixture of ZnO and Zn_2TiO_4 was investigated by ^{67}Zn MAS NMR. **Fig. 2a** shows the spectrum of the initial sintered mixture, recorded at a magnetic field of B_0 = 19.6 T with natural abundance of ^{67}Zn nuclei. The signals at δ_{67Zn} = 75 ppm and 231 ppm were assigned to the Zn_2TiO_4 and ZnO phases of the pellets, respectively. The integrated areas of the two peaks and spinning sidebands (*) were approximately

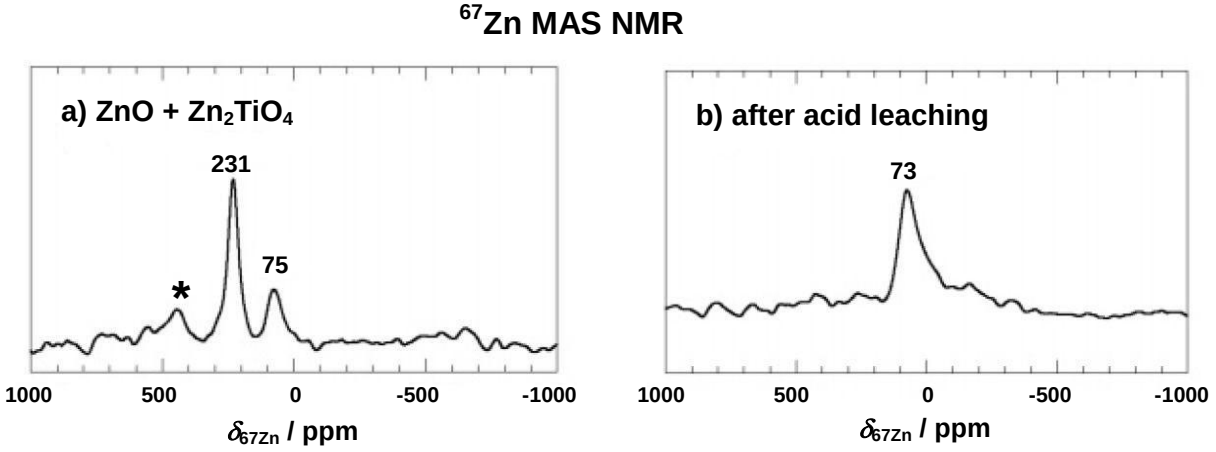

Fig. 2

consistent with their relative Zn stoichiometry and mole ratio. After acid leaching, the ZnO signal δ_{67Zn} = 231 ppm completely disappeared, while the signal at δ_{67Zn} = 73 ppm indicated the presence of a slightly modified Zn_2TiO_4 phase (**Fig. 2b**). Due to the complete ZnO leaching, the modified Zn_2TiO_4 pellets contain macropores, suitable for applications in adsorption processes and heterogeneous catalysis [5].

The doping of ZnO nanoparticles with aluminum was investigated in Ref. [6]. In this study, surface-enhanced spectroscopy via indirect DNP (dynamic nuclear polarization, see "method 23" and Ref. [7]) transfer was utilized for recording ^{67}Zn solid-state NMR spectra of Zn species near the particle surface (**Fig. 3**). During CW (continuous wave) irradiation, an enhanced electron polarization (e^-) of TEKPol polarizing agents (Fig. 3 in "method 23") is obtained. For reaching a high $e^- \rightarrow {}^1$H polarization transfer within the TEKPol molecules, the DNP experiment is performed at low temperature (T = 105 K).

$e^- \rightarrow {}^1$H $\rightarrow {}^{67}$Zn polarization pathway

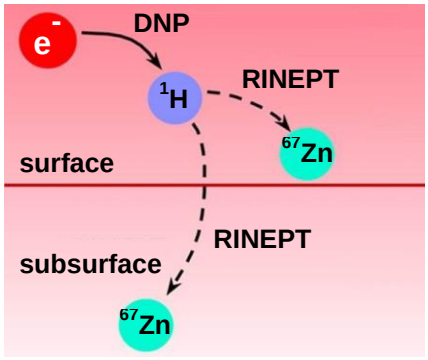

Fig. 3

Upon $e^- \rightarrow {}^1$H polarization transfer, the DNP-enhanced polarization of the ^{1}H nuclei of the TEKPol molecules is transferred to surface-near ^{67}Zn nuclei via the RINEPT (refocused insensitive nuclei enhanced by polarization transfer, see Ref. [8]) method (**Fig. 4**). Via this pulse group, decoupling of ^{1}H-^{1}H interactions improves the efficiency of the polarization transfer from ^{1}H nuclei to ^{67}Zn nuclei. Additionally, the hetero-nuclear dipolar ^{1}H-^{67}Zn recoupling sequence $SR4_1^2$(tt) [9] with low t1-noise [10] is applied. In the channel of the ^{67}Zn nuclei, a QCPMG (quadrupolar Carr-Purcell-Meiboom-Gill, see "method 17") sequence is irradiated. The ^{67}Zn MAS NMR

spectrum is obtained by Fourier transformation of the sum of the QCPMG echoes. For further details, see Ref. [6].

$^{1}H \rightarrow {}^{67}Zn$ RINEPT-SR4$_1^2$(tt)-QCPMG pulse group

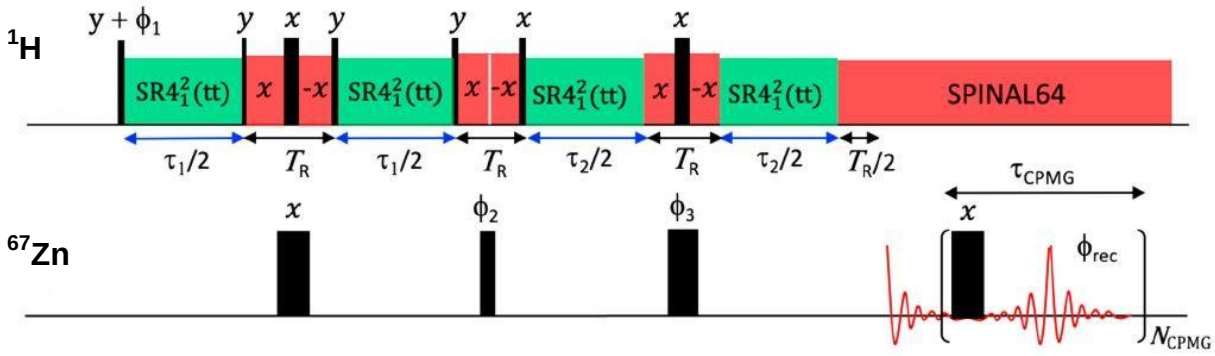

Fig. 4

The ^{67}Zn solid-state NMR spectrum of Al-doped ZnO particles in **Fig. 5a** was recorded by indirect DNP-enhanced $^{1}H \rightarrow {}^{67}Zn$ RINEPT-SR4$_1^2$(tt) NMR spectroscopy [6]. This spectrum was recorded at a magnetic field of B_0 = 9.4 T and using MAS with a sample spinning frequency of ν_{rot} = 10 kHz. The most intense ^{67}Zn solid-state NMR

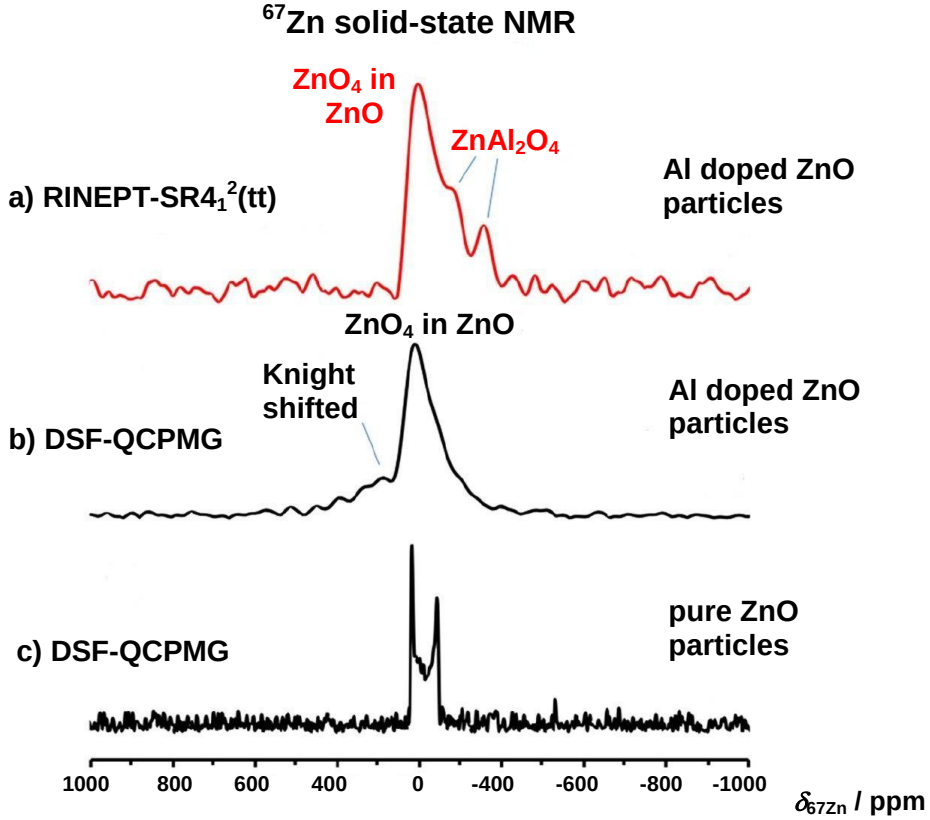

Fig. 5

signal occurs at δ_{iso} = 236.9 ppm and was simulated with a quadrupole coupling constant of C_Q = 2.38 MHz according to ZnO_4 sites in ZnO [6]. Two weak high-field signals were explained by $ZnAl_2O_4$ phases, in which a fraction of Zn^{2+} ions substitutes the Al^{3+} ones in octahedral sites [6]. These signals are absent in the DFS-QCPMG (double frequency sweep [11]) spectrum in **Fig. 5b**, which indicates that the amount of $ZnAl_2O_4$ phases is small and exclusively located near the surface of the Al-doped ZnO particles. The ^{67}Zn DFS-QCPMG NMR spectrum of pure ZnO in **Fig. 5c** agrees with those of other studies, such as the spectrum in **Fig. 1b**.

The metal-organic framework (MOF) MOF-5 in **Fig. 6a**, with a large surface area of approximately 4.000 m^2/g, is one of the most widely studied MOF compounds [12]. It possesses large cubic cavities, which are initially filled with solvent molecules. The oxygen-centered Zn_4O tetrahedra of Zn-MOF-5 at each corner of the cubes are connected by 1,4-benzendicarboxylate (BDC) ligands as organic linkers (see also Fig. 3 in "method 5"). The solvent molecules, e.g. chloroform, can be completely removed from the framework by either solvent extraction or heat treatment while the framework still maintains its integrity [12].

The static ^{67}Zn spin-echo NMR spectrum of the partially desolvated MOF-5 (8.2 wt.% guest molecules) in **Fig. 6b, top,** was recorded at a magnetic field of B_0 = 21.1 T. The simulation yielded the presence of single Zn sites with C_Q = 3.4 MHz and η_Q = 0.40 [12]. The further desolvation of the MOF-5 sample caused a broadening of the corresponding static ^{67}Zn spin-echo NMR spectrum (**Fig. 6b, bottom)** hinting at significant changes in the Zn coordination environment. The spectrum could be

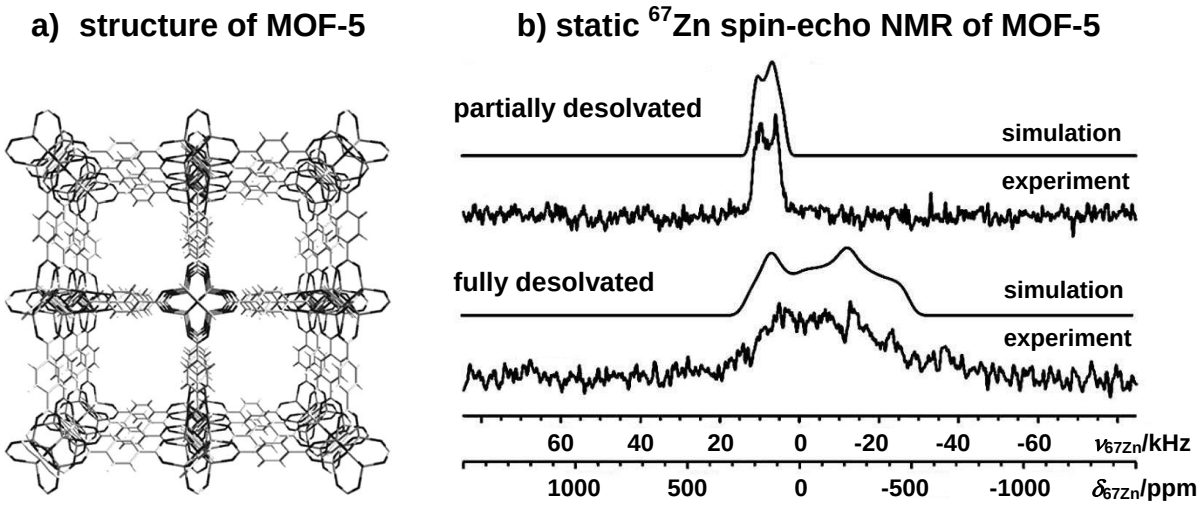

Fig. 6

simulated by single Zn sites of C_Q = 7.4 MHz and η_Q = 0.40 [12]. The much larger C_Q value indicates that the distortion in the local Zn environment in fully desolvated samples is significantly stronger than in partially desolvated MOF-5.

Within the MOF family, the zeolite-imidazolate framework (ZIF) of type ZIF-8 is among the most promising ZIF materials, due to the high potential of this material for applications in hydrocarbon separation, notably of alkanes and alkenes [13]. First ^{67}Zn MAS NMR studies of ZIF-8, ZIF-14, ZIF-7 and ZIF-4 were described in Ref. [12]. In Ref. [13], ZIF-8 samples before and after adsorption of an ethane/ethane mixture (1:1) were investigated. The ^{67}Zn MAS NMR spectrum of the unloaded ZIF-8 was explained by tetrahedrally coordinated Zn sites. Only a slight change of the isotropic chemical shift from δ_{67Zn} = 297 ppm for the unloaded to δ_{67Zn} = 294 ppm for the ethane/ethane-loaded material was observed. This finding indicates that the ethane/ethane adsorption on ZIF-8 does not remarkably influence the coordination of Zn atoms inside the structure [13]. For pure Zn(imidazole)$_4$(ClO$_4$)$_2$, an isotropic chemical shift of δ_{67Zn} = 291 ppm was determined [14]. For further ^{67}Zn solid-state NMR studies of Zn-MOFs and similar materials, see Refs. [15] and [16].

The high catalytic activity of Zn-containing zeolites led to intensive studies on the activation of lower alkanes, particularly methane (see e.g. Ref. [17]). For clarifying the active-site synergy arising from the spatial interaction of acidic hydroxyl groups and Zn^{2+} atoms in Zn^{2+}/ZSM-5 zeolites, double-resonance ^{1}H–^{67}Zn solid-state NMR studies were performed [18, 19]. The Zn-modified ZSM-5 (n_{Si}/n_{Al} = 21) zeolites under study, contained 2 wt.% (ZSM-5(I2)) and 6 wt.% (ZSM-5(I6)) Zn atoms, prepared by incipient wetness impregnation. The NMR spectroscopic studies were performed at a magnetic field of B_0 = 18.8 T utilizing the sensitivity enhanced HS-QCPMG (hyperbolic secant-(quadrupolar Carr-Purcell-Meiboom-Gill) NMR technique [20]. To further improve the NMR sensitivity, ^{67}Zn (89.6%) enriched precursors were used for the preparation of the Zn-modified zeolites by impregnation with ^{67}Zn-labeled zinc acetate.

In the ^{67}Zn HS-QCPMG NMR spectra of ZSM-5(I6) and ZSM-5(I2) in **Fig. 7a, top and middle**, two signals with isotropic chemical shifts of δ_{67Zn} = 238 ppm and 224 ppm occur [18, 19]. The signal at δ_{67Zn} = 238 ppm was assigned to ZnO species, which was supported by the spectrum of ZnO/ZSM-5 in **Fig. 7a, bottom**. The lacking quadrupolar line shape in the spectra of ZSM-5(I6) and ZSM-5(I2) indicates the occurrence of highly dispersed ZnO particles on ZSM-5. The signal at δ_{67Zn} = 224

ppm has a much larger linewidth and was assigned to Zn^{2+} ions located on the cation exchange sites of ZSM-5. The asymmetry in the local structure of Zn species induced by the zeolite framework may lead to an increase of quadrupolar interaction, which results in the line broadening and high-field shift. Based on the results of additional ^{1}H-{^{67}Zn} S-RESPDOR (symmetry-based resonance-echo double-resonance) NMR investigations [21], the local structure of Zn^{2+} species in ZSM-5 with the ^{1}H-^{67}Zn atom-atom distances depicted in **Fig. 7 b** was suggested [18, 19].

a) ^{67}Zn HS-QCPMG NMR of ZSM-5 **b) local structure of Zn^{2+} in ZSM-5**

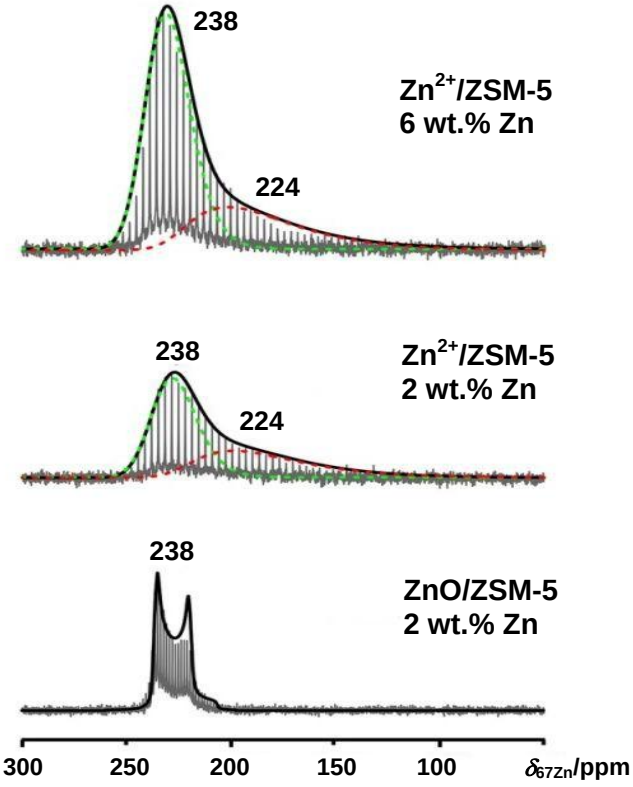

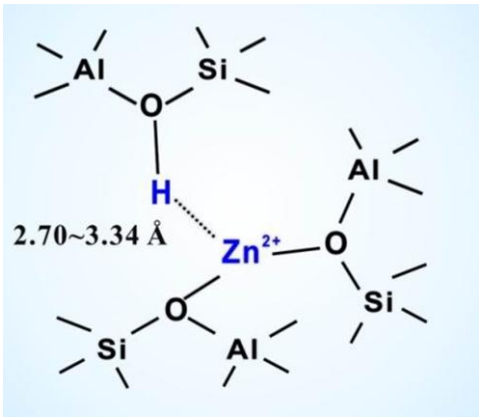

Fig. 7

In Ref. [22], ^{67}Zn solid-state NMR studies of two ZSM-5 zeolites prepared by solid-state exchange (T = 773 K for 7 h) with ^{67}Zn-enriched (90 %) zinc powder (Zn^{2+}/ZSM-5) and by ion exchange with ^{67}Zn-enriched (90%) zinc formate solution (ZnO/H-ZSM-5), both containing ca. 3.8 wt.% Zn, are described. One of the reasons of this investigation was to quantify the different Zn species observable by ^{67}Zn MAS NMR spectroscopy at a magnetic field of B_0 = 17.6 T. **Fig. 8** shows the ^{67}Zn MAS NMR spectra of pure ZnO powder (a), utilized as intensity reference, hydrated Zn^{2+}/ZSM-5 (b), hydrated ZnO/H-ZSM-5 (c), and activated (T = 773 K for 7 h) ZnO/H-ZSM-5 (d).

The height of spectrum (a) was reduced by a factor of ten with respect to the other spectra.

The spectrum of hydrated Zn^{2+}/ZSM-5 (**Fig. 8b**) exhibits exclusively a signal in the region of δ_{67Zn} = 0 ppm belonging to octahedrally coordinated (ZnO_6) zinc species. The activated ZnO/H-ZSM-5 (**Fig. 8d**) shows exclusively a signal in the region of tetrahedrally coordinated Zn species (ZnO_4). The spectrum of hydrated ZnO/H-ZSM-5 (**Fig. 8c**) exhibits signals of both tetrahedrally (ZnO_4) and octahedrally coordinated zinc species (ZnO_6). No ^{67}Zn MAS NMR signals were observed for the activated Zn^{2+}/ZSM-5 zeolite. By simulation, quadrupole coupling constants of $C_Q \cong 2.5$ MHz for the ZnO_4 signals and $C_Q \cong 3.0$ MHz for the ZnO_6 signals in **Figs. 8b to 8d** were estimated [22].

Quantitative ^{67}Zn MAS NMR analysis using the ZnO powder as reference has shown that only 38% and 27% of the zinc atoms on hydrated and activated ZnO/H-ZSM-5, respectively, are visible. For hydrated Zn^{2+}/ZSM-5, 24% of the zinc atoms were found to be visible by ^{67}Zn MAS NMR spectroscopy [22]. The signal of octahedrally coordinated zinc species and the signal of ZnO specie were explained by hydrolysis of the bonds of Zn^{2+} cations with the oxygen atoms of the zeolite framework and further hydration of the formed $[HOZn]^+$ cations or $Zn(OH)_2$ species

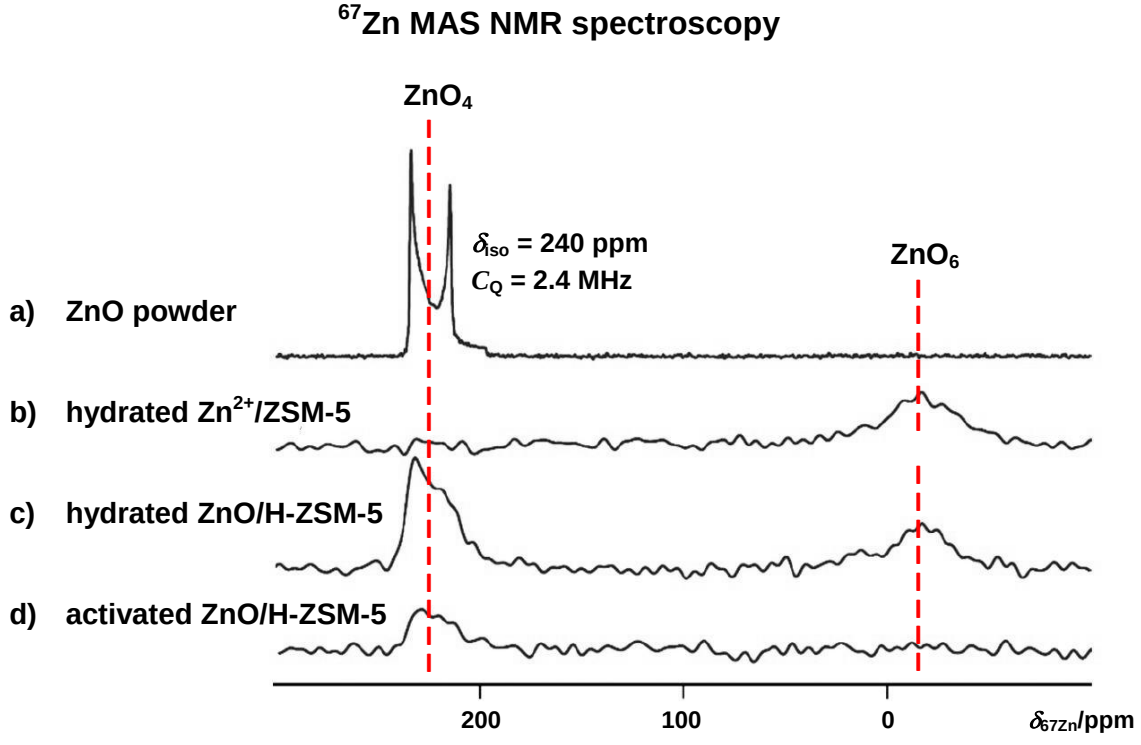

Fig. 8

with water molecules. The obtained $[HOZn(H_2O)_5]^+$ cations or $[(H_2O)_4Zn(OH)_2]$ species are suggested to be visible by ^{67}Zn MAS NMR spectroscopy at B_0 = 17.6 T. While the ^{67}Zn MAS NMR spectrum of activated Zn^{2+}/ZSM-5 zeolite exhibits no signal, the hydration of this zeolite leads to the formation of $[HOZn(H_2O)_5]^+$ cations, which are visible by ^{67}Zn MAS NMR spectroscopy. The invisible zinc atoms were explained by Zn species with asymmetric local structures leading to quadrupole coupling constants of C_Q > 20 MHz [23, 24]. In this case, a line broadening by 25 times and a corresponding decrease in the signal amplitude must be expected [22], making such Zn species invisible by ^{67}Zn MAS NMR spectroscopy at B_0 = 17.6 T.

In **Table** 1, a survey on ^{67}Zn solid-state NMR parameters of zinc species in zeolites, zeolite-like materials and reference materials is given.

For a general overview on the recent state of solid-state NMR spectroscopy of low-γ nuclei, see Ref. [25].

Materials and Zn Species	**δ_{iso}/ppm**	**C_Q / MHz**	**η_Q**	**Refs.**
ZnS, cubic, (ZnS_4)	380.5	0	0.0	[1]
	378	0	0.0	[26]
ZnS, hexagonal, (ZnS_4)	365	< 0.5	0	[1]
	364.5	< 0.4	0	[2]
$Zn(thiourea)_4(NO_3)_2$, (ZnS_4)	358	3.15	1.0	[27]
Zn-MOF-5 partially desolvated		3.4	0.4	[12]
completely desolvated		7.4	0.4	[12]
Zn-MOF ZIF-7 (ZnN_4)	260-320	6.2	0.95	[12]
Zn-MOF ZIF-4 (ZnN_4) Zn site 1		5.0	0.25	[12]
Zn site 2		3.8	0.75	[12]
Zn-MOF ZIF-8 (ZnN_4)	297			[13]
		1.1	0.8	[12]
$Zn(imidazole)_4(ClO_4)_2$, (ZnN_4)	291	2.8	0.4	[27]
$K_2Zn(CN)_4$, cubic, (ZnC_4)	291	0		[28]
ZnSe, cubic, ($ZnSe_4$)	273			[26]
	276			[27]

Zn-MOF ZIF-14 (ZnN_4)	260	2.8	0.85	[12]
$Zn(CH_3COOH)_2$, (ZnO_4)	245	2.4	0.1	[27]
ZnO, hexagonal,(ZnO_4)	240 232	2.4	0.0	[1], [2] [5]
ZnTe, cubic, ($ZnTe_4$)	87.6			[1]
Zn_2TiO_4, cubic, (ZnO_4 and ZnO_6)	65			[5]
$ZnSO_4 \cdot 7H_2O$, (ZnO_6)	10	1.70	0.2	[2]
$Zn(CH_3COOH)_2 \cdot 2H_2O$, ($ZnO_6$)	0	5.3	0.85	[14]
$Zn(ClO_4)_2 \cdot 6H_2O$, (ZnO_6)	-3.0	< 0.2		[27]

Table 1

Sample preparation: The ZnO powder used for recording the spectra in **Fig. 1** was commercially available and studied without any additional preparation [2].

Pellets consisting of a mixture of ZnO and Zn_2TiO_4 particles, utilized for the studies of **Fig. 2**, were prepared at a pressure of ca. 1.6×10^3 kg cm^2. Subsequently, the pellets were fired in air at T = 1473 K for 12 h in a covered alumina crucible [5].

The aluminum-doped ZnO powder and the ZnO microcrystalline powder, utilized for recording the spectra in **Fig. 5**, were purchased from Sigma-Aldrich [6].

The metal-organic framework MOF-5 used for recording the spectra in **Fig. 6b** was synthesized as described in detail in the Supporting Information of Ref. [12].

The Zn^{2+}/ZSM-5 (n_{Si}/n_{Al} = 21) samples with 6 and 2 wt.% Zn, prepared for the studies in **Fig. 7**, were obtained by incipient wetness impregnation of the parent zeolite with ^{67}Zn-labeled zinc acetate solution, followed by drying at T = 373 K for 16 h and further calcination at T = 773 K for 6 h in air [18]. The ZnO/ZSM-5 sample with 2 wt.% Zn was prepared by mechanical mixing of ^{67}Zn-labeled zinc oxide with H-ZSM-5 ($n_{Si}/\underline{n}_{Al}$ = 21) by grinding at room temperature [18].

The Zn^{2+}/ZSM-5 zeolite, used for recording the spectrum in **Fig. 8b**, was prepared by the reaction of activated ZSM-5 zeolite ($n_{Si}/\underline{n}_{Al}$ = 13) and metallic zinc with n_{Zn}/n_{Al} = 5 at T = 773 K for 7 h in a vacuumed glass ampule [22]. The ZnO/ZSM-5 zeolite used for recording the spectra in **Fig. 8c** and **Fig. 8d** was obtained by an ion exchange of the parent ZSM-5 zeolite with zinc formate solution ($^{67}Zn(HCOO)_2$) [22].

^{67}Zn solid-state NMR studies: The spectra in **Fig. 1** were recorded at a resonance frequency of ν_0 = 25.036 MHz (B_0 = 9.4 T), with a pulse width of 5 µs and using recycle delays of 0.5 to 1.0 s. The spectra in **Fig. 1a** and **Fig. 1b** were obtained upon 31772 and 9536 scans, respectively [2].

The ^{67}Zn MAS NMR measurements for **Fig. 2** were performed on a Bruker DRX-830 spectrometer at ν_0 = 51.92 MHz (B_0 = 19.6 T) and with a sample spinning rate of ν_{rot} = 10 kHz [5].

All ^{67}Zn solid-state NMR spectra in **Fig. 5** were recorded on a Bruker BioSpin Avance NEO DNP-NMR spectrometer at B_0 = 9.4 T, equipped with a double resonance H/X 3.2 mm low-temperature MAS probe [6]. The DNP-enhanced RINEPT-SR4$_1^2$(tt) NMR spectrum in **Fig. 5a** was obtained with the same spectrometer, except that a 263 GHz gyrotron for enhancing the electron polarization (e^-) of the TEKPol polarizing agents at low temperature was additionally used [6]

The ^{67}Zn solid-state NMR experiments leading to the spectra in **Fig. 6b** were conducted on a Bruker Avance II spectrometer at B_0 = 21.1 T, operating at ν_0 = 56.4 MHz. The static ^{67}Zn NMR spectra were acquired with proton decoupling (decoupling field of 25 kHz) by using the Hahn-echo pulse sequence [(π/2)-τ-(π)-τ-acq with τ = 20 to 50 ms on a homebuilt 7 mm H/X low-γ NMR probe [12].

The ^{67}Zn HS-QCPMG NMR spectra of Zn-containing ZSM-5 zeolites in **Fig. 7a** were recorded on a Bruker AvanceIII 800 spectrometer, with a resonance frequency of ν_0 = 50.07 MHz, at a magnetic field of B_0 = 18.8, and using a 4 mm HX low-γ probe at a sample spinning rate of ν_{rot} = 10 kHz. The HS-QCPMG experiment was optimized using natural abundance pure ZnO powder [18, 19].

The ^{67}Zn MAS NMR spectra of Zn-containing ZSM-5 zeolites in **Fig. 8** were obtained on a Bruker AVANCE 750 spectrometer at a resonance frequency of ν_0 = 47 MHz, a magnetic field of B_0 = 17.6 T, and with a high-power Bruker probe and a MAS frequency of ν_{rot} = 10 kHz [22].

^{67}Zn chemical shifts were referenced to an aqueous solution of 1.0 M $Zn(NO_3)_2$ (δ_{iso} = 0 ppm).

References:

[1] T.J. Bastow, S.N. Stuart, *NMR study of the zinc chalcogenides (ZnX, X = 0, S, Se, Te)*, Phys. Stat. Sol. 146 (1988) 719-728, DOI: 10.1002/pssb.2221450238.

[2] G. Wu, *Zinc-67 nuclear magnetic resonance spectroscopy of solids*, Chem. Phys. Lett. 298 (1998) 375-380, DOI: 10.1016/S0009-2614(98)01237-8.

[3] G. Spataro, Y.Champouret, P. Florian, Y. Coppel, M.L. Kahn, *Multinuclear solid-state NMR study: A powerful tool for understanding the structure of ZnO hybrid nanoparticles*, Phys. Chem. Chem. Phys. 20 (2018) 12413-12421, DOI: 10.1039/c8cp01096j.

[4] R. Ohashi, W. Sato, M. Mizuno, S. Ohki, K. Deguchi, M. Tansho, T. Shimizu, *Investigation of the effects of sintering and indium-doping of zinc oxide using ^{67}Zn magic angle spinning NMR analysis*, Solid State Nucl. Magn. Reson. 95 (2018) 12-16, DOI: 10.1016/j.ssnmr.2018.09.001.

[5] E.S. Toberer, J.D. Epping, B.F. Chmelka, R. Seshadri, *Hierarchically porous rutile titania: Harnessing spontaneous compositional change in mixed-metal oxides*, Chem. Mater. 18 (2006) 6345-6351, DOI: 10.1021/cm0621693.

[6] H. Nagashima, J. Trebosc, Y. Kon, K. Sato, O. Lafon, J.-P. Amoureux, *Observation of low-γ quadrupolar nuclei by surface-enhanced NMR spectroscopy,* J. Am. Chem. Soc. 142 (2020) 10659-10672, DOI: 10.1021/jacs.9b13838.

[7] A.G.M. Rankin, J. Trebosc, F. Pourpoint, J.-P. Amoureuxa, O. Lafon, *Recent developments in MAS DNP-NMR of materials*, Solid State Nucl. Magn. Reson. 101 (2019) 116-143, DOI: 10.1016/j.ssnmr.2019.05.009.

[8] R. Zhang, A. Ramamoorthy, *Performance of RINEPT is amplified by dipolar couplings under ultrafast MAS conditions*, J. Magn. Reson. 243 (2014) 85-92, DOI: 10.1016/j.jmr.2014.03.012.

[9] H. Gu, L. Liang, D. Wu, X. Yao, G. Hou, *Windowed symmetry pulses for enhanced heteronuclear dipolar recoupling in solid-state MAS NMR*, Precis. Chem. 5(6) (2026) 811-820, DOI: 10.1021/prechem.5c00364.

[10] F.A. Perras, T. Wei Goh, W. Huang, *t1-noise elimination by continuous chemical shift anisotropy refocusing*, Solid State Nucl. Magn. Reson. 120 (2022) 101807, DOI: 10.1016/j.ssnmr.2022.101807.

[11] Y.T.A. Wong, M. Negroni, A.P.M. Kentgens, *Enhancing half-integer quadrupolar solid-state NMR signals via steady states: A double frequency sweep-based approach*, J. Chem. Phys. 162 (2025) 094202, DOI: 10.1063/5.0249863.

[12] A. Sutrisno, V.V. Terskikh, Q. Shi, Z. Song, J. Dong, S.Y. Ding, W. Wang, B.R. Provost, T.D. Daff, T.K. Woo, Y. Huang, *Characterization of Zn-containing metal-organic frameworks by solid-state ^{67}Zn NMR spectroscopy and computational modeling*, Chem. Eur. J. 18 (2012) 12251-12259, DOI: 10.1002/chem.201201563.

[13] D. Freude, N. Dvoyashkina, S.S. Arzumanov, D.I. Kolokolov, A.G. Stepanov, C. Chmelik, H. Jin, Y. Li, J. Kärger, J. Haase, *NMR study of the host structure and guest dynamics Investigated with alkane/alkene mixtures in metal organic frameworks ZIF-8*, J. Phys. Chem. C 123 (2019) 1904-1912, DOI: 10.1021/acs.jpcc.8b11673.

[14] A.C. Kunwar, G.L. Turner, E. Oldfield, *Solid-state spin-echo Fourier transform NMR of ^{39}K and ^{67}Zn salts at high field*, J. Magn. Reson. 69 (1986) 124-127, DOI: 10.1016/0022-2364(86)90224-6.

[15] R.S. K. Madsen, A. Qiao, J. Sen, I. Hung, K. Chen, Z. Gan, S. Sen, Y. Yue, *Ultrahigh-field ^{67}Zn NMR reveals short-range disorder in zeolitic imidazolate framework glasses*, Science 367 (2020) 1473-1476, DOI: 10.1126/science.aaz0251.

[16] W. Zhang, A. Hassan, J. Struppe, M. Monette, I. Hung, Z. Gan, V. Martins, V. Terskikh, Y. Huang, *Overcoming challenges in ^{67}Zn NMR: A new strategy of signal enhancement for MOF characterization*, Chem. Commun. 59 (2023) 5205-5208, DOI: 10.1039/d3cc00716b.

[17] A.A. Gabrienko, S.S. Arzumanov, M.V. Luzgin, A.G. Stepanov, V.N. Parmon, *Methane activation on Zn^{2+}-exchanged ZSM-5 zeolites. The effect of molecular oxygen addition*, J. Phys. Chem. C 119 (2015) 24910-24918, DOI: 10.1021/acs.jpcc.5b08759.

[18] G. Qi, Q. Wang, J. Xu, J. Trebosc, O. Lafon, C. Wang, J.-P. Amoureux, F. Deng, *Synergic effect of active sites in zinc-modified ZSM-5 zeolites as revealed by high-field solid-state NMR spectroscopy*, Angew. Chem. Int. Ed. 55 (2016) 15826-15830, DOI: 10.1002/anie.201608322.

[19] J. Xu, Q. Wang, F. Deng, *Metal active sites and their catalytic functions in zeolites: Insights from solid-state NMR spectroscopy*, Acc. Chem. Res. 52 (2019) 2179-2189, DOI: 10.1021/acs.accounts.9b00125.

[20] R. Siegel, T. T. Nakashima, R. E. Wasylishen, *Signal enhancement of NMR spectra of half-integer quadrupolar nuclei in solids using hyperbolic secant pulses*, Chem. Phys. Lett. 388 (2004) 441-445, DOI: 10.1016/j.cplett.2004.03.047.

[21] L. Chen, Q. Wang, B. Hu, O. Lafon, J. Trebosc, F. Deng, J.-P. Amoureux, *Measurement of hetero-nuclear distances using a symmetry-based pulse sequence in solid-state NMR*, Phys. Chem. Chem. Phys. 12 (2010) 9395-9405, DOI: 10.1039/b926546e.

[22] M. Avramovska, D. Freude, J. Haase, A.V. Toktarev, S.S. Arzumanov, A.A. Gabrienko, A.G. Stepanov, *Quantitative ^{67}Zn, ^{27}Al and ^{1}H MAS NMR spectroscopy for the characterization of Zn species in ZSM-5 catalysts*, Phys. Chem. Chem. Phys. 25 (2023) 28043-28051, DOI: 10.1039/d3cp03136e.

[23] Y. Huang, A. Sutrisno, *Recent advances in solid-state ^{67}Zn NMR studies: From nanoparticles to biological systems*, Annu. Rep. NMR Spectrosc. 81 (2014) 1-46, DOI: 10.1016/B978-0-12-800185-1.00001-2.

[24] A.S. Lipton, C. Bergquist, G. Parkin, P.D. Ellis, *Solid-state ^{67}Zn NMR spectroscopic studies and ab initio molecular orbital calculations on a synthetic analogue of carbonic anhydrase*, J. Am. Chem. Soc. 125 (2003) 3768-3772, DOI: 10.1021/ja021328q.

[25] M.E. Smith, *Recent progress in solid-state nuclear magnetic resonance of half-integer spin low-γ quadrupolar nuclei applied to inorganic materials*, Magn. Reson. Chem. 59 (2021) 864-907, DOI: 10.1002/mrc.5116.

[26] M. Haller, W.E. Hertler, O. Lutz, A. Nolle, *^{67}Zn and ^{33}S nuclear magnetic shielding in zinc chalcogenides*, Solid State Commun. 33 (1980) 1051-1053, DOI: 10.1016/0038-1098(80)90315-4.

[27] S. Sham, G. Wu, *Zinc-67 NMR study of tetrahedral and octahedral zinc sites with symmetrical oxygen, nitrogen, and sulfur ligands*, Can. J. Chem. 77 (1999) 1782-1787, DOI: 10.1139/v99-154.

[28] G. Wu, S. Kroeker, R.E. Wasylishen, *Multinuclear NMR study of dipotassium tetracyanometalates of the group 12 metals in the solid state*, Inorg. Chem. 34 (1995) 1595-1598, DOI: 10.1021/ic00110a043.